Hydrogeol J
DOI 10.1007/s10040-016-1410-2

REPORT

The effects of a dry sand layer on groundwater recharge in extremely arid areas: field study in the western Hexi Corridor of northwestern China

Peng Sun[1] · **Jinzhu Ma**[1] · **Shi Qi**[1] · **Wei Zhao**[1] · **Gaofeng Zhu**[1]

Received: 18 October 2015 / Accepted: 23 March 2016

Abstract Evaporation capacity is an important factor that cannot be ignored when judging whether extreme precipitation events will produce groundwater recharge. The evaporation layer's role in groundwater recharge was evaluated using a lysimeter simulation experiment in the desert area of Dunhuang, in the western part of the Hexi Corridor in northwestern China's Gansu Province. The annual precipitation in the study area is extremely low, averaging 38.87 mm during the 60-year study period, and daily pan evaporation amounts to 2,486 mm. Three simulated precipitation regimes (normal, 10 mm; ordinary annual maximum, 21 mm; and extreme, 31 mm) were used in the lysimeter simulation to allow monitoring of water movement and weighing to detect evaporative losses. The differences in soil-water content to a depth of 50 cm in the soil profile significantly affected rainfall infiltration during the initial stages of rainfall events. It was found that the presence of a dry 50-cm-deep sand layer was the key factor for "potential recharge" after the three rainfall events. Daily precipitation events less than 20 mm did not produce groundwater recharge because of the barrier effect created by the dry sand. Infiltration totaled 0.68 mm and penetrated to a depth below 50 cm with 31 mm of rainfall, representing potential recharge equivalent to 1.7 % of the rainfall. This suggests that only extreme precipitation events offer the possibility of recharge of groundwater in this extremely arid area.

✉ Jinzhu Ma
jzma@lzu.edu.cn

[1] Key Laboratory of Western China's Environmental Systems (Ministry of Education), College of Earth and Environmental Sciences, Lanzhou University, 222 South Tianshui Road, Lanzhou 730000, China

Keywords Groundwater recharge · Unsaturated zone · Rainfall · Dry sand layer · China

Introduction

Water scarcities are common in semiarid and arid regions because of the limited water supply and increasing demand created by population growth and inappropriate development planning (Vörösmarty et al. 2000). As a result, the total global groundwater depletion in sub-humid to arid areas has increased from 126 km^3 $years^{-1}$ in 1960 to 283 km^3 $years^{-1}$ in 2000 as a result of increased groundwater abstraction; the problem is especially severe in the world's major agricultural regions, which include northwestern India, northern China, and the central United States (Wada et al. 2010). Overall, shallow groundwater exists in 22–32 % of the world's land area (Fan et al. 2013), but these resources are at risk when groundwater abstraction exceeds the rate of recharge. The renewal capacity of the groundwater system, which is a key parameter in determining the sustainable yield of systems that depend on this water, depends strongly on the aquifer recharge rate. Approximately 24.5 % of China's land is located in the arid and semiarid areas of northwestern China, where precipitation is sufficiently low enough that it contributes little to groundwater recharge, and this area has been severely affected by desertification. Sandy deserts and desertified land cover an estimated 1.49×10^6 km^2 of the landmass of China, or about 15.5 % of the total land area (Wang et al. 2004). Thus, it is urgently necessary to quantify the current rate of groundwater recharge in these dry areas to support efforts to manage the groundwater resource sustainably, since this resource is critical for economic development.

Knowledge of the infiltration of precipitation and the resulting groundwater recharge is essential to rational

Published online: 16 April 2016

planning and management of an arid region's groundwater resource (Ma et al. 2009a). Recent studies have suggested that precipitation is the key factor responsible for groundwater recharge in desert systems (Ma and Edmunds 2006), but it remains unclear whether heavy rain events produce effective infiltration that results in recharge (Chen et al. 2014; Dong et al. 2013; Ma et al. 2014). Much of the water contributed by precipitation runs off or evaporates instead of joining the regional groundwater system (De Vries and Simmers 2002). Based on the observations of matrix-distributed lysimeters, at least 91 % of the precipitation in the Hexi Desert evaporates before it can recharge groundwater (Xu et al. 1998); the rest remains in the sand layer at depths from 0 to 40 cm. This suggests that sand layers play an important role in the soil-water distribution, and cannot be ignored in studies of groundwater recharge. Chen et al. (2014) conducted a continuous observation of water contents in the sand layer in the Badain Jaran Desert after two rainfall events, and found that 10.6 and 25 mm of precipitation infiltrated to depths of 13 and 40 cm, respectively; however, this water evaporated within 15 days. Based on these results, they hypothesized that even extreme precipitation events may not recharge groundwater. Dong et al. (2013) performed an artificial precipitation experiment in the Badain Jaran Desert and found that 30 mm of precipitation was unable to infiltrate deep enough to recharge the groundwater. Ma et al. (2014) noted that precipitation could not always infiltrate deeply enough into the soil to recharge the groundwater even when the precipitation exceeded 40 mm. Despite these negative results, deserts have been shown to experience good recharge of groundwater based on historical reconstructions, although the recharge rates were small, accounting for an annual average of 0.2–5 % of the rainfall (Edmunds et al. 2006; Gates et al. 2008; Ma et al. 2009b, 2012; Scanlon et al. 2010). These results raise the important question of whether extreme rainfall events might produce groundwater recharge in desert systems (Chen et al. 2014). The quantity of potential recharge from rainfall depends strongly on the rainfall intensity, and the relationship between these two factors has been studied in detail (Liu et al. 2015; Huang et al. 2013; Schindewolf and Schmidt 2012). The role of the dry sand layer appears to be particularly important in determining the potential recharge (Brutsaert 2014; Wang et al. 2006, 2008, 2015; Wen et al. 2014).

A dry sand layer forms in the surface layers of a bare, sandy soil during drying of the soil, and within this layer, soil moisture is present predominantly in the vapor phase and the soil-water potential is usually less than -1.5×10^4 cm (Goss and Madliger 2007). Such a layer can create an important barrier to vapor flow, what Wang (2015) referred to as "vapor flow resistance", that affects the soil water's evaporation rate and dynamic processes under natural conditions (Ahn et al. 2012; Shahraeeni et al. 2012; Swenson and Lawrence 2014). In other words, the dry sand layer can retard further drying of the underlying soils (Wang 2015). Drainage or percolation to a depth below the root zone (or below the dry sand layer in a bare soil) is termed "potential recharge", and has been equated to the eventual recharge that occurs at the water table (Scanlon et al. 2010). The concept of potential recharge is important for modeling future groundwater conditions (De Vries and Schwan 2000; De Vries and Simmers 2002; De Vries et al. 2000). The deserts located in extremely arid areas have an annual precipitation less than 50 mm, with a low frequency of rainfall events, and this makes it difficult to explore the influence of the dry sand layer on the potential recharge after different types of rainfall events. In these water-limited regions, the bare soil, soil-water flows, and climate are strongly coupled (Shurbaji and Campbell 1997); however, there is no strong consensus on the effects of the dry sand layer on precipitation infiltration, evaporation, and groundwater recharge. The objective of the present study was to evaluate the effect of the dry sand layer on groundwater recharge by means of a simulation experiment with a large lysimeter under different rainfall events. The specific goals were (1) to analyze the moisture redistribution processes that occur in a bare desert soil in response to different rainfall events; and (2) to simulate the barrier effect of the dry sand layer on groundwater recharge based on a water balance equation under different rainfall events. The study was conducted in the Dunhuang region, an extremely arid part of northwestern China.

Study area

Dunhuang (39.55°N–40.05°N, 94.25°E–94.48°E) is located in the western part of the Hexi Corridor in northwestern China's Gansu Province (Fig. 1), and is an important part of the ancient Silk Road (Ma et al. 2013). The study area is bounded by the Mazong Mountains to the north, the Danghe Reservoir to the south, and the Danghe River valley to the east, with a north–south width of 20 km and an east–west length of 40 km. The region is adjacent to the Qinghai-Tibetan plateau, and the elevation ranges between 800 and 1,650 m asl. Dunhuang's position at the western end of the Hexi Corridor places it in a tectonic zone that belongs to the Dunhuang Basin, in the western part of the Shulehe Basin. The soil is composed of early Quaternary sediments above the Jiuquan gravel layer (Fig. 1c). Unconsolidated Quaternary sediments that reach thicknesses of hundreds of meters were deposited in the southern foreland, reaching thicknesses of tens of metres at the edge of the basin. Together, these sediments form significant unconfined and confined groundwater systems. In the western part of the Dunhuang Irrigation District and near the urban area, the alluvial and diluvial aquifer is formed of highly permeable cobbles, gravels, and sands in a layer ranging from 200 to 400 m in thickness. Interbedding of the gravel and sand layers occurs

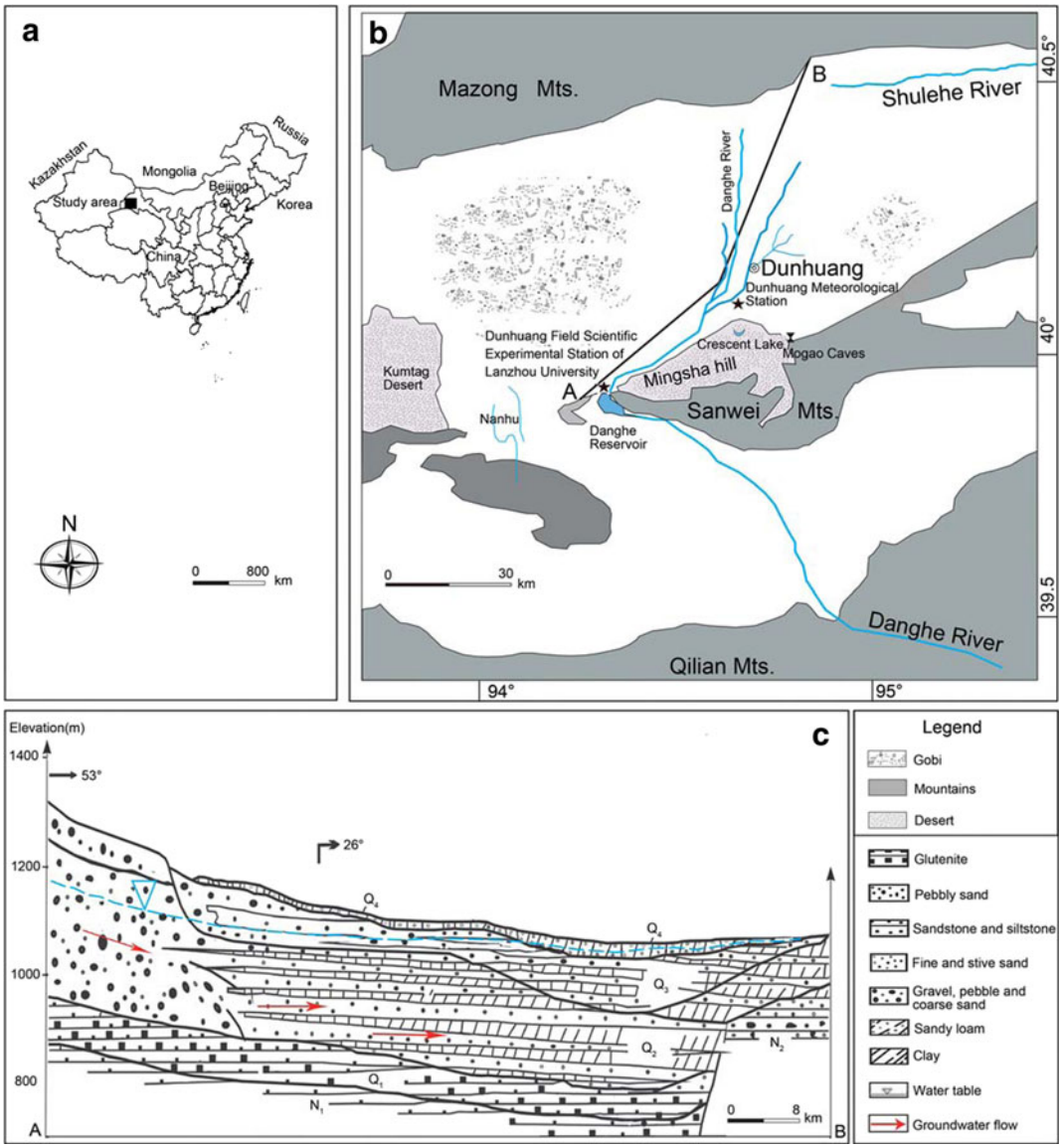

Fig. 1 **a** Map of China with the location of the study area. **b** Geographical and hydrological features of the Dunhuang Basin, showing the location of the Field Scientific Experimental Station of Lanzhou University and Dunhuang Meteorological Station. **c** Hydrogeological cross-section (from point *A* to point *B*) through the Dunhuang Basin

between the mountains and the riverbed terraces, with the deposits mainly composed of modern river alluvial materials covered by aeolian sand (Ma et al. 2013).

Based on data from 1954 to 2014 obtained from the Dunhuang Meteorological Station, which is located at the northern edge of the Mingsha Mountains, the mean annual temperature is 9.6 °C, with the recorded extremes ranging from a maximum of 43.6 °C in July to a minimum of −28.6 °C in January. The temperature range between the minimum and maximum mean monthly values is 34 °C. The mean annual precipitation averages only 38.87 mm, which represents hyper-arid conditions. The rainfall is concentrated in the period from April to September, which accounts for 83 % of the total annual precipitation. The average relative humidity in Dunhuang is less than 40 %, and the sunshine duration totals 3,200 h annually, with an annual total solar radiation of 6,418.4 MJ m^{-2}. The near-surface wind speed averages 3 m s^{-1} annually, with winds strong enough to entrain sand occurring on an average of 89 days $year^{-1}$. The dominant sand-entraining winds flow from the west and northwest. The average annual potential evaporation is 2,486 mm. The natural vegetation community is dominated by shrubs (primarily *Nitraria tangutorum* and *Tamarix ramosissima*) and grasses (primarily *Achnatherum splendens* and *Artemisia argyi*). The soil surface is mostly bare, with the surface sediments dominated by mobile to semi-mobile dunes.

Experimental methods

Experimental conditions and equipment

The simulated rainfall experiments were carried out at the Dunhuang Field Scientific Experimental Station of Lanzhou University (39.9°N, 94.35°E), which is 2.4 km from the Mingsha hills (Echoing Sand Mountain; Fig. 1). Figure 2 illustrates the experimental setup used during the simulated rainfall events in the summer of 2014. A portable rainfall simulation device (RS-6, UGT, Muncheberg, Germany) was used to accurately control the rainfall amount and intensity. The rainfall simulator has two main components: (1) The water supply and simulation control system provides the desired water supply using a rainfall controller that maintains the rainfall uniformity as high as possible; (2) the swing nozzle produces a uniform distribution of raindrops. The water tank used in this study had a 2-L capacity. To prevent errors introduced by natural rainfall, the lysimeter was covered by a shelter (Fig. 2a) during the period when simulated rainfall was supplied, but the shelter was subsequently removed to eliminate interference with natural evaporation (e.g., to avoid blocking winds and solar radiation). To prevent small-scale topographic variations from influencing the results, the soil surface was leveled before the experiment began.

These components are paired with a lysimeter that allows monitoring of water movement and weighing to detect losses to evaporation. The lysimeter (L-07W lysimeter system, Xian Bishui Water Environment Technology Company, Xian, China) was paired with a data-acquisition system. The soil box used in the experiments was $2.0 \times 2.0 \times 2.8$ m^3 and contained three soil layers (Fig. 3). The sandy soils used in the lysimeter were obtained from a site near the Mingsha Mountains and were mixed thoroughly to increase their homogeneity.

Table 1 summarizes the physical properties of the soil. The evaporation rates were determined by the weighing lysimeter system at 10-min intervals, with an accuracy of ±0.1 kg,

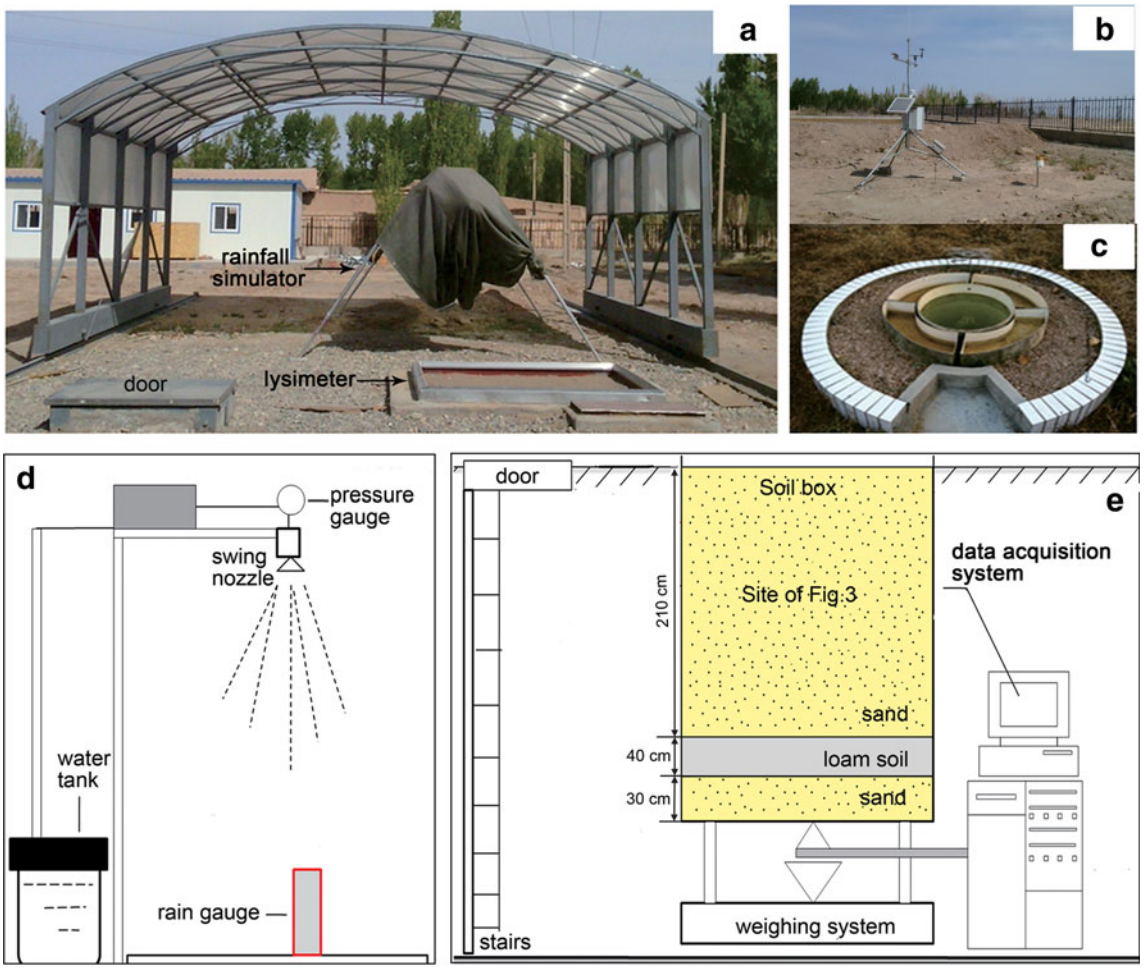

Fig. 2 **a** View of the experimental system including the rainfall simulator and lysimeter. **b** The recording meteorological station used to monitor environmental characteristics during the study. **c** The E-601 evaporation pan, which was used to estimate the pan evaporation. **d** The structure and components of rainfall simulator. **e** The lysimeter soil box (site of Fig. 3) with the data-acquisition system and weighing system. The soil comprised a layer of sand above and below a layer of loam soil

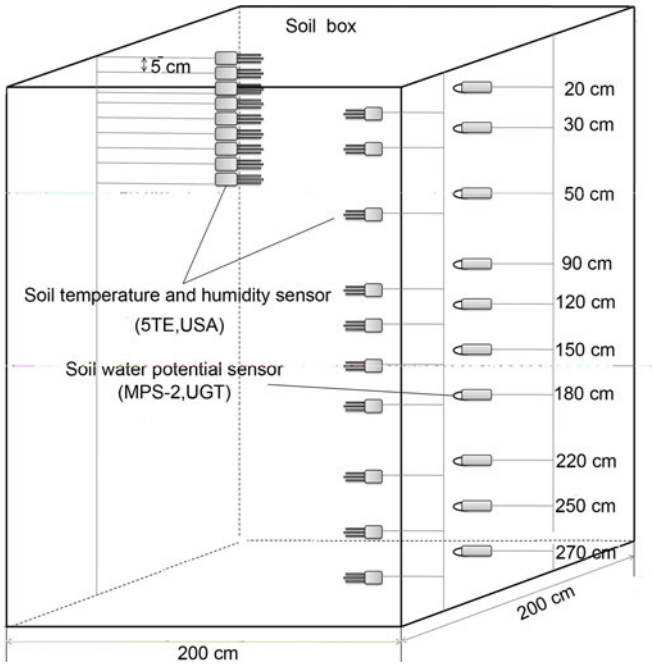

Fig. 3 Soil box showing the locations of the sensors. Note that measurements were obtained at 5-cm intervals between the surface and a depth of 50 cm

during the experimental session.The soil temperature and moisture data were measured using a soil temperature and moisture sensor (5TE, Decagon Devices, Pullman, WA, USA) paired with a soil-water potential sensor (MPS-2; Decagon Devices). Water contents, temperatures, and water potentials were measured at 10-min intervals at 5-cm intervals from the surface to a depth of 50 cm, and then at 10 additional depths in the soil profile (Fig. 3), with precisions of ±0.0008 m^3 m^{-3}, ±0.5 °C, and ±0.01 MPa, respectively. The initial volumetric soil-water content (SWC) of the layers, before beginning the experiments, ranged from 1.8 to 11.7 %. Table 2 summarizes the precision and accuracy of the main instruments.

Continuous complementary measurements included standard climatological data, recorded using an automatic meteorological station (Vantage Pro, Davis Instruments, San Francisco, CA, USA). Air temperature and relative humidity were measured at 2 m above the ground. Wind speed and total solar radiation were measured at 3 m above the ground. All parameters were observed at 0.5-h intervals. During the experimental session, the daily pan evaporation was measured using a free-water evaporation pan (E-601, Dayu Hydrological Science and Technology Company, Weifang, Shandong Province, China).

Rainfall simulations

Based on the precipitation characteristics at Dunhuang from 1954 to 2014, three simulated precipitation regimes were developed (Table 3): 10 mm (normal), 21 mm (ordinary annual maximum), and 31 mm (extreme). The following principles were used to design these treatments: (1) rainfall events were concentrated during the summer rainy season; (2) the individual rainfall simulations were conducted for a duration of 1 week; (3) the precipitation characteristics agreed with the characteristics of local modern precipitation (from 1954 to 2014); and (4) the precipitation intensity was approximately equal in the three treatments.

The increase in soil moisture in each layer during rainfall events was calculated based on the principle of soil-water balance (Huang et al. 2013; Wang et al. 2008). Because of the dense layout of the sensors in

Table 1 Physical properties of the soil in the lysimeter

Bulk density (g cm^{-3})	Porosity	Particle-size distribution (%)				Saturated moisture content (%)
		Clay (<0.15 mm)	Fine sand (0.15–0.2 mm)	Medium sand (0.2–0.5 mm)	Coarse sand (>0.5 mm)	
1.6	0.36	4.035	26.082	58.325	11.558	35

Table 2 The precision and accuracy of the instruments for data recorded at the study site. *SWC* volumetric soil-water content

Instruments	Units	Instrument model	Measurement range	Precision	Validation method	Accuracy
Rainfall simulator	mm	RS–6	5–125	±0.1	Rain gauge	±0.1
SWC	$m^3\ m^{-3}$	5TE	0–0.5	±0.0008	Laboratory measurement	±0.002
Lysimeter	kg	LW–07	0–2000	±0.1	Small weighing lysimeter	±0.3

this study, it was possible to accurately monitor infiltration of the water. The following equation (Wang et al. 2008) was used to calculate the cumulative infiltration (i.e., the amount of water that penetrates to a depth where it will not evaporate):

$$I_s = \frac{1}{10}(\theta_{end} - \theta_f) \cdot \Delta h \quad (1)$$

where I_s is the cumulative infiltration (mm), θ_{end} is the volumetric soil-water content ($m^3\ m^{-3}$) at the end stage, θ_f is the initial volumetric soil-water content ($m^3\ m^{-3}$), and Δh is the thickness of the soil layer soil depth interval (cm); the value of 10 converts the result from cm to mm.

Evaporation estimates and measurements of the dry sand layer

Evaporation also plays a key role in the water cycle in desert systems. The potential evaporation was calculated using the data collected by the evaporation pan (ET_{pan}). The value of this parameter is determined by the soil texture (e.g., coarse vs. fine sands), solar radiation, relative humidity, and other factors (Xie and Wang 2007). Reference evapotranspiration, denoted as ET_0, can be calculated using the FAO-56 calculation method (Allen et al. 1998), with a 60-day measurement period. Many previous studies have shown that the dry surface sand inhibits evaporation, and the intensity of this effect is closely related to the thickness of this layer. The thickness of the dry sand layer was measured according to the method of Yamanaka and Yonetani (1999) with a caliper by excavating the soil surface at noon every day. The bottom boundary of the dry sand layer can be visually distinguished from the underlying soil layer by a color contrast (Fritton et al. 1967; Yamanaka et al. 1997; Yamanaka and Yonetani 1999).

Results

Characteristics of precipitation and evaporation

To analyze the long-term precipitation characteristics, the daily precipitation data from 1954 to 2014 recorded at the Dunhuang Meteorological Station (40.15°N, 94.68°E) were used. Figure 4 presents the distribution of mean annual precipitation and rainfall events from 1954 to 2014. The annual precipitation in the study area is extremely low, with a mean of 38.87 mm during the 60-year period. The range of annual precipitation is also high: from 6.4 to 105.1 mm. Precipitation per rainfall event is mostly less than 10 mm, accounting for 96.6 % of all rainfall events (Table 4).

Figure 4b,d present the daily rainfall and its frequency. These data suggest three kinds of precipitation events (Table 4): (1) "normal" precipitation represents a total daily precipitation of <10 mm, which accounted for 96.6 % of the rainfall events recorded in the study area from 1954 to 2014; (2) "ordinary annual maximum" precipitation represents daily precipitation between 10 and 30 mm, which accounts for 3.4 % of the rainfall events; (3) "extreme" precipitation represents rainfall events greater than 30 mm, which occurred only twice from 1954 to 2014. These amounts and frequencies are similar to those previously reported for the Badain Jaran Desert (Ma et al. 2014).

Although mean annual precipitation averaged 38.87 mm, ordinary annual maximum precipitation events and extreme precipitation events sometimes occurred. Because these events were rare (less than 4 % of the total events), infiltration of water was dominated by the normal events, but the other types of events may still have had an influence on the groundwater and its recharge. Unfortunately, because of the rarity of the latter events, it was necessary to perform a simulated rainfall experiment in the study to compare the effects of the different rainfall events.

Figure 5 shows the daily reference evapotranspiration (ET_0, mm) and daily potential evaporation (ET_{pan}, mm). ET_0

Table 3 Characteristics of the three individual rainfall events used as the experimental treatments from 1 June to 1 September 2014

Event No.	Date (year/month/day)	Precipitation (mm)	Rainfall duration (h)	Rainfall intensity ($mm\ h^{-1}$)	Type	Probability of occurrence (‰)
M1	2014.06.03	10 (±0.5)	0.5	20.0	Normal	25.0
M2	2014.06.10	21 (±0.4)	1.0	21.0	Ordinary annual maximum	5.0
M3	2014.07.22	31 (±0.6)	1.5	20.7	Extreme	0.2

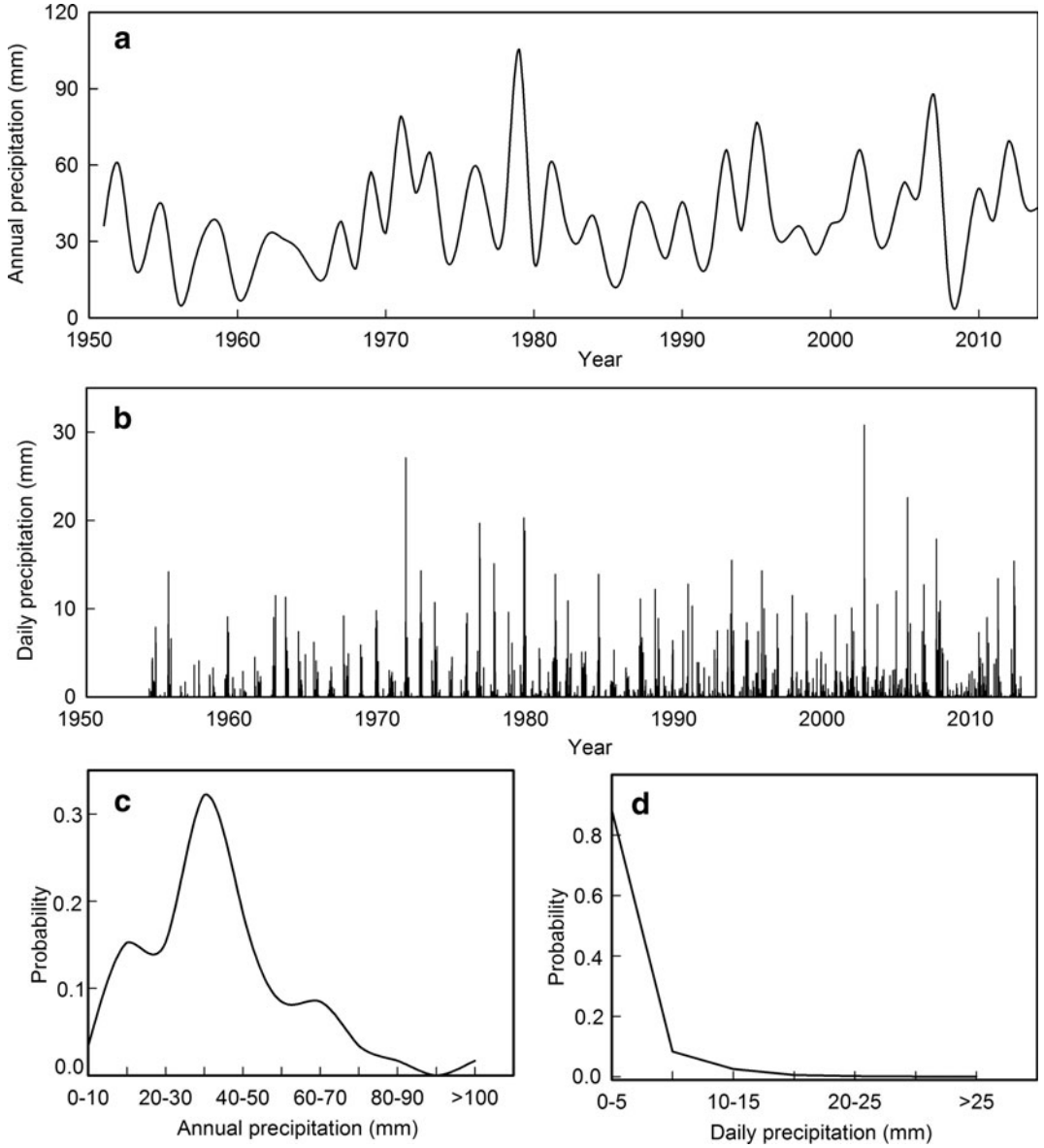

Fig. 4 Average annual precipitation (**a**), daily precipitation (**b**) in the Dunhuang basin from 1954 to 2014, and frequency of annual precipitation (**c**) and frequency of daily precipitation (**d**)

and ET_{pan} were 1,086 and 2,486 mm, respectively. The strongest evaporation occurred from approximately day of year (DOY) 110 to 240, a period of approximately 4 months from 10 April to 1 September that corresponds to the growing season. During this period, ET_0 reached a maximum of slightly more than 4 mm and ET_{pan} reached a maximum of slightly more than 11 mm, which were both far higher than the average daily precipitation of 1.9 mm (including only days when a rainfall event occurred).

Wetting front in the dry sand layer

Figure 6 shows the changes in soil-water content at different depths in the lysimeter's soil box during the three precipitation simulations. In the normal rainfall simulation (Fig. 6a), with 10.0 mm of precipitation, infiltration caused SWC at a depth of 5 cm to increase rapidly and then stabilize, whereas SWC increased slowly but steadily at a depth of 10 cm and did not change at a depth of 15 cm. In the ordinary annual maximum rainfall event (Fig. 6b), with 21 mm of precipitation, there was a similar pattern, with the SWC changing rapidly at shallow depths and then increasing more gradually with increasing depth, but infiltration reached a depth of 30 cm. In the extreme rainfall event simulation (Fig. 6c), with 31 mm of precipitation, a more rapid increase occurred at shallower depths and infiltration continued to occur to a depth of 50 cm.

Figure 7 shows the position of the wetting front as a function of the infiltration time. This result shows that the greater

Table 4 Frequency distribution for daily rainfall and consecutive rainfall events for the three precipitation categories (normal, ordinary annual maximum, and extreme) based on data from 1954 to 2014 at the Dunhuang Meteorological Station

Rainfall events		Normal		Ordinary annual maximum		Extreme	
		<5 mm	5–10 mm	10–20 mm	20–30 mm	>30 mm	Total
Daily rainfall events	No.	488	32	15	1	0	536
	Frequency	64.64	4.24	1.99	0.13	0	70.99
Consecutive rainfall last 2 days	No.	104	28	12	3	0	152
	Frequency	13.77	3.71	1.56	0.39	0	20.13
Consecutive rainfall last 3 days	No.	22	6	4	3	0	35
	Frequency	2.91	0.79	0.53	0.39	0	4.64
Consecutive rainfall last 4 days	No.	9	8	7	1	0	25
	Frequency	1.19	1.06	0.93	0.13	0	3.31
Consecutive rainfall last more than 5 days	No.	1	0	3	1	2	7
	Frequency	0.13	0	0.39	0.13	0.26	0.92

the rainfall amount and duration, the deeper the water penetrates and the faster it reaches a given depth (i.e., the steeper the slope of the curve). Based on these results, the infiltration in the homogeneous surface sandy soil appears to be a piston flow. For the normal precipitation, the wetting front reached a depth of only 10 cm, and it took 50 min for the water to reach this depth. This is similar to the results reported in other deserts in arid areas of northwestern China (Ma and Edmunds 2006; Ma et al. 2009b). Based on the frequency of normal rainfall events (Table 4), this suggests that 92.4 % of the rainfall events in the study area have a negligible impact on potential recharge because of the thick barrier represented by the surface dry sand layer. For the ordinary annual maximum rainfall, with a rainfall amount from 10 to 30 mm, the water infiltrated deeper into the soil (i.e., it reached a depth of 25 cm after 90 min with 21 mm of precipitation), which suggests that these rainfall events also

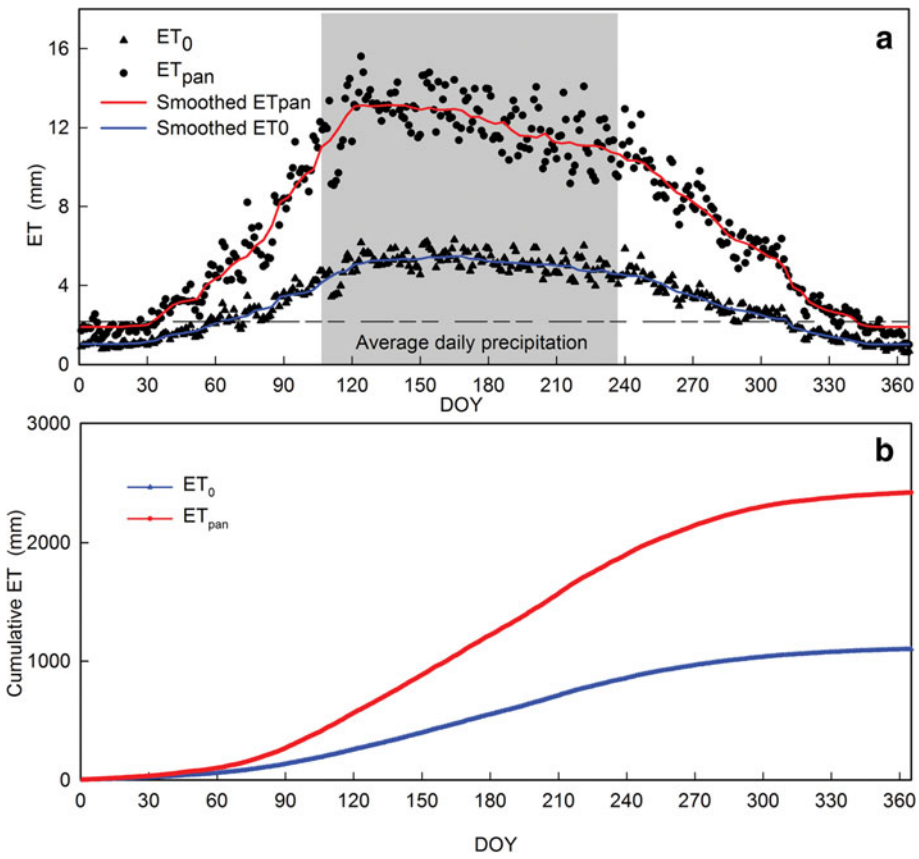

Fig. 5 The average daily reference evapotranspiration (ET_0), daily pan evaporation (ET_{pan}) (**a**), and cumulative evaporation (**b**) in the Dunhuang region as a function of the day of year (*DOY*). The *shaded area* represents the growing season. The *horizontal dashed line* represents the average daily precipitation

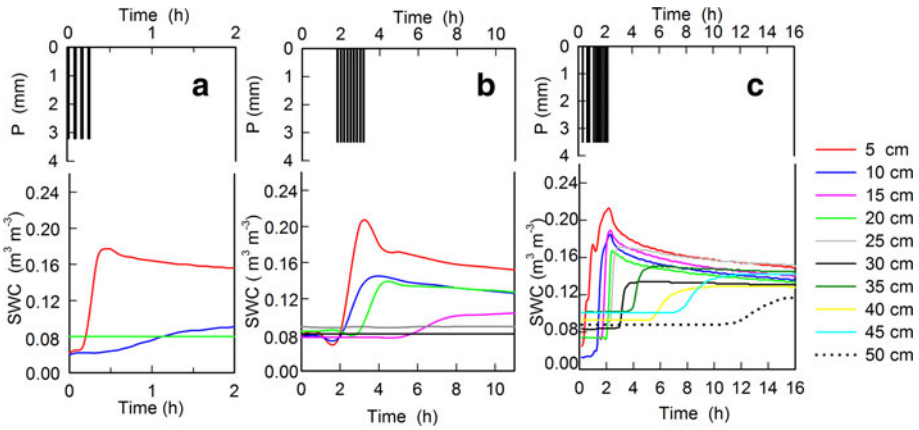

Fig. 6 Changes in volumetric soil-water content (*SWC*) at 10 depths in the lysimeter's soil box during water infiltration after simulated rainfall events, and the rainfall intensity during the experiment period (Table 4): **a** normal precipitation, **b** ordinary annual maximum precipitation, and **c** extreme precipitation

provide a less significant contribution to the potential recharge if the thickness of the surface dry sand layer is greater than 25 cm. For extreme rainfall events, with 31.0 mm of rain, the wetting front reached a depth of 50 cm after 720 min, suggesting that it may contribute to the potential recharge if the surface dry sand layer is shallower than 50 cm.

Quantity, duration, intensity, and temporal distribution are the key factors that influence the quantity and process of water infiltration into the deep soil (Liu et al. 2011; Yang et al. 2014). Regression analysis of the relationship between the infiltration depth (D) and infiltration duration (t) revealed the following results:

$$10\text{ mm of rain: } D = 10.39 - 10.39\ \exp(-0.065t),\ R^2 = 0.9998,\ p < 0.05$$
$$21\text{ mm of rain: } D = 28.71 - 29.16\ \exp(-0.024t),\ R^2 = 0.9966,\ p < 0.05$$
$$31\text{ mm of rain: } D = 49.62 - 45.42\ \exp(-0.005t),\ R^2 = 0.9793,\ p < 0.05$$

During the experimental period from 1 June to 1 September 2014, four natural rainfall events occurred. The total rainfall amounted to 4.68 mm, with a total duration of less than an hour (Table 5). These rainfall events, with a maximum rainfall intensity of 10.05 mm h^{-1} and an average intensity of 4.22 mm h^{-1}, would only reach a depth of 5 cm from the surface after the largest rainfall event (3.35 mm). Combined with the results of the simulated rainfall, this suggests that normal rainfall only affected the soil moisture content to a depth of 10 cm, and that soil moisture in deeper layers was not affected by 92.4 % of the rainfall events in this study area.

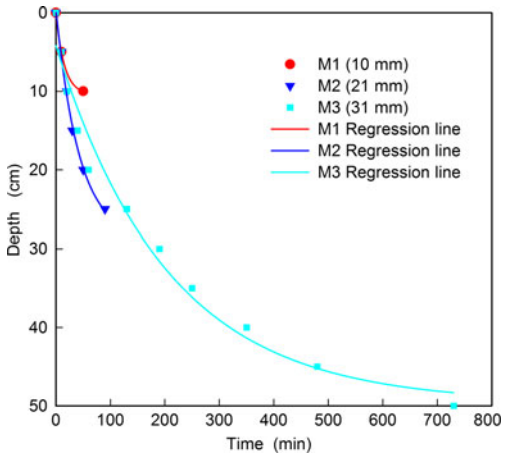

Fig. 7 The position of the wetting front as a function of time in the simulated rainfall events in the surface sand layer. Precipitation characteristics for events *M1–M3* are summarized in Table 3

Soil-water profiles

Figure 8 shows the timing and rainfall amount for the simulated and natural rainfall events and the resulting changes in SWC at depths ranging from 5 to 50 cm below the surface of the sand layer. The layer from 0 to 5 cm showed the most sensitive response to rainfall, and the only differences was that the magnitude of the fluctuation in SWC response to the amount of rainfall events; in particular, for natural rainfall, the variation in SWC was nearly undetectable. In the layers at 10, 20, and 30 cm, SWC showed no response to the four natural rainfall events. With ordinary annual maximum rainfall (Fig. 8), the response of the SWC decreased with increasing depth and became undetectable at depths below 30 cm. Thus for both normal and ordinary annual maximum rainfall, the presence of a dry surface sand layer prevented water infiltration below a depth of 30 cm. With extreme rainfall (31 mm), increases in SWC were detectable even at a depth of 50 cm. Thus, extreme rainfall events create a possibility of potential recharge of the groundwater (De Vries and Simmers 2002), although the recharge quantity may be small.

Figure 9 shows the changes in soil-water content with depth as a result of rainfall infiltration into the soil after three rainfall events. The rainfall amount has a much more important impact than the initial conditions on the depth of water infiltration. Soil-water content at 10 cm depth had greater difference between before and after the rainfall event M1;

Table 5 Four natural rainfall events during the experiment period from 1 June to 1 September 2014

Event No.	Date (year/month/day)	Precipitation (mm)	Rainfall duration (min)	Rainfall intensity (mm h^{-1})	Type	Depth of infiltration (cm)
N1	2014.06.18	0.50	10	3.00	Normal	<5
N2	2014.06.27	3.35	20	10.05	Normal	5
N3	2014.08.20	0.58	15	2.32	Normal	<5
N4	2014.08.21	0.25	10	1.50	Normal	<5

however, soil-water content from 20 to 50 cm depth increased only slightly, and no significant differences were found before or after rainfall. Significant differences were also found in soil-water content at the 0–30 cm depths before and after the event M2, and for soil-water content from 30 to 50 cm depth no significant differences were found. Additionally, soil-water content from 0 to 50 cm depth increased quickly after the event M3. In the subsequent period of 300 days of no precipitation, the SWC showed rising trend on the depths 90 and 120 cm (Fig. 9, M3), and the wetting front could reach 120 cm depth. As a result, it can continue moving downwards and potentially recharge the groundwater.

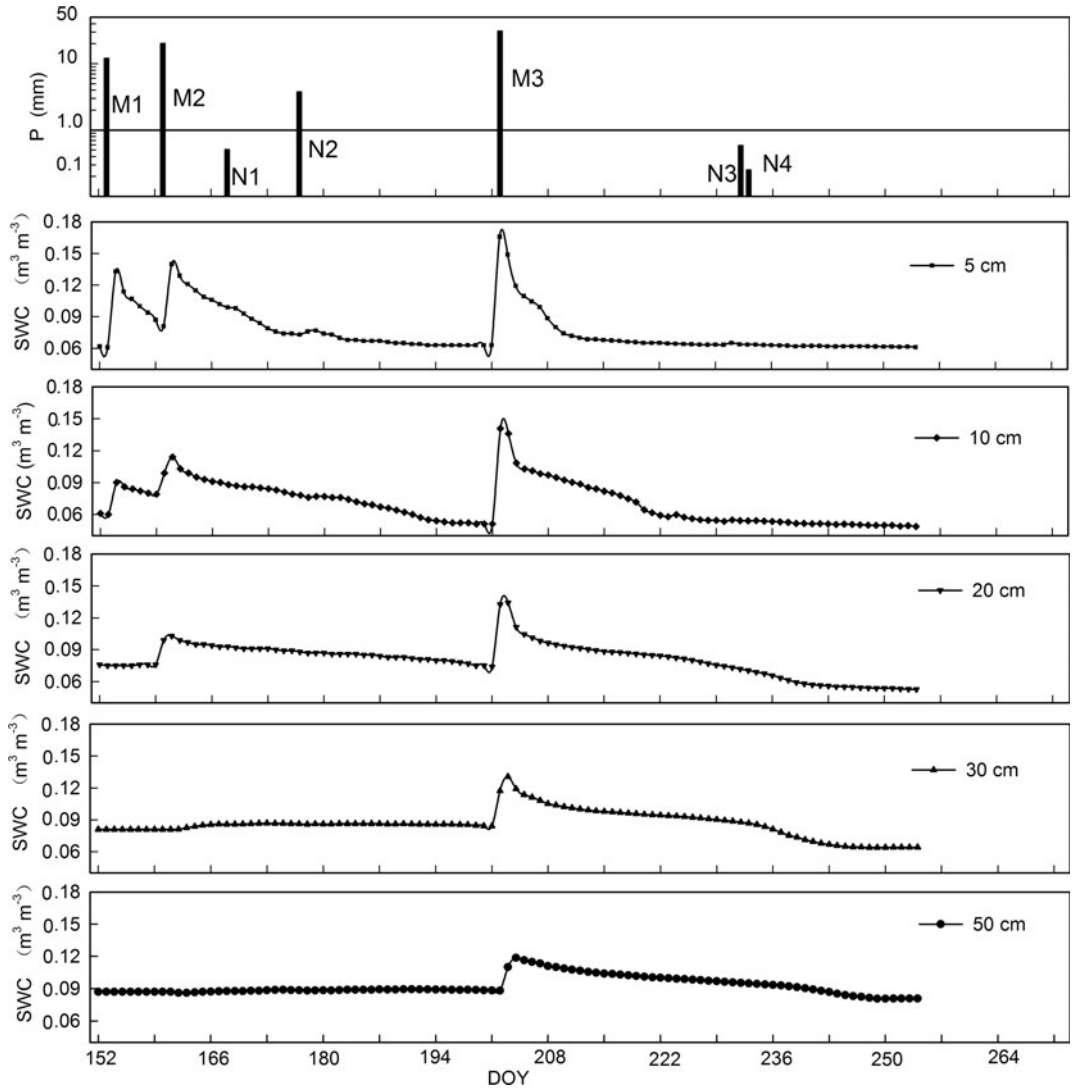

Fig. 8 Timing and rainfall amount of the simulated (*M1–M3*; Table 3) and natural (*N1–N4*; Table 5) rainfall events, and the resulting changes in soil-water content (*SWC*) at depths of *5–50* cm in the soil. Rainfall descriptions: *M1*, simulated 10-mm rainfall; *M2*, simulated 21-mm rainfall; *M3*, simulated 31-mm rainfall; *N1–N4*, natural rainfall ranging from 0.25 to 3.35 mm

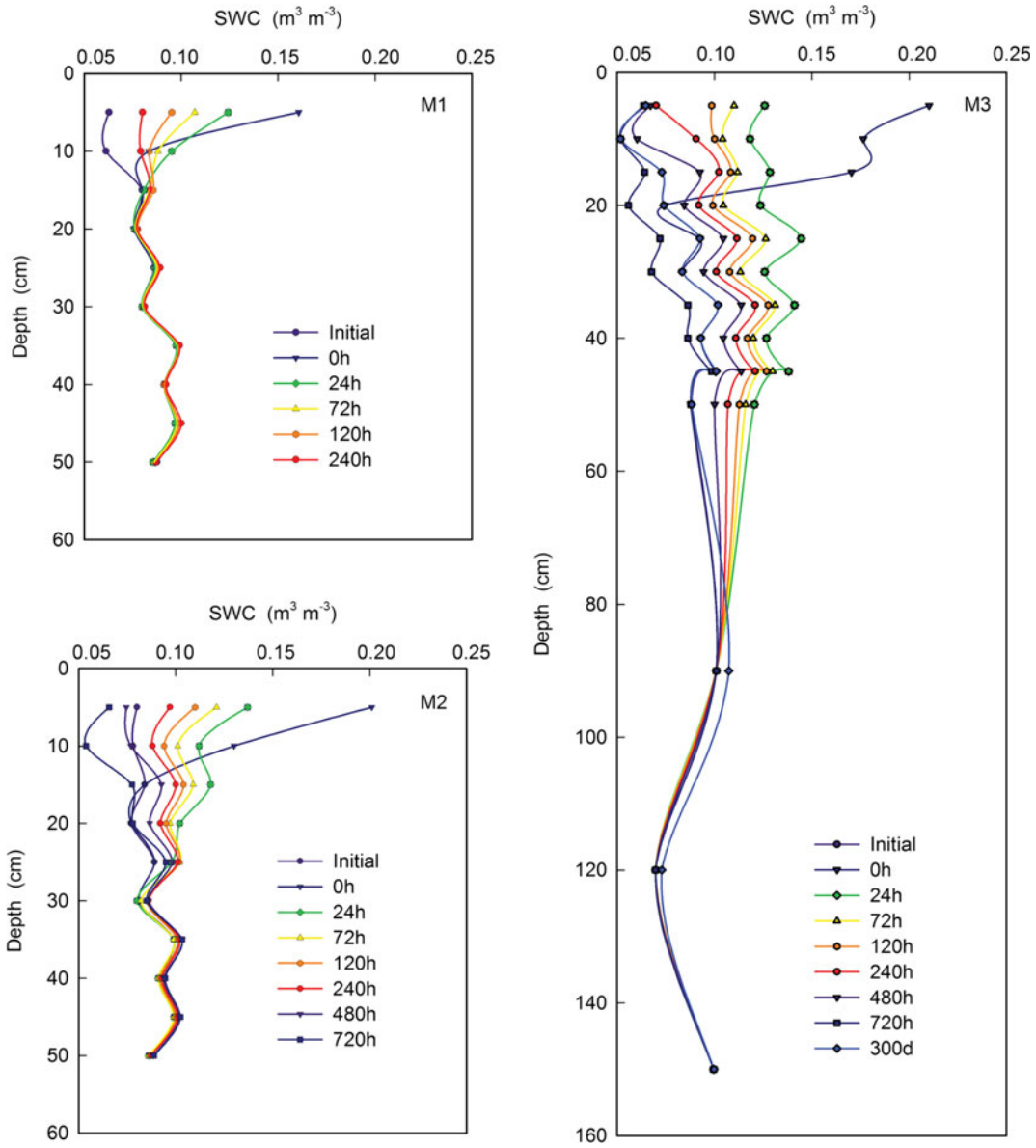

Fig. 9 Successive soil-water profiles in soil column at different times (hours) following simulated rainfall events of *M1–M3*

Evaporation and moisture loss

Rainfall, infiltration, and evaporation are the key components of the water cycle in desert systems in the extremely arid areas of northwestern China (Wu 2009), and evaporation is particularly important. Figure 10 shows the cumulative and daily actual and pan evaporation during the experimental period. In addition to the barrier to infiltration created by the dry surface sand layer, the high evaporation rate makes it more difficult for water to infiltrate to great depths; the daily pan evaporation capacity averaged 7.2 mm during the experimental period, which is larger than all of the natural rainfall events and comparable to the normal simulated rainfall amount. Cumulative pan evaporation increased at a relatively stable rate during the experimental period, reaching 488 mm after 72 days, whereas the actual evaporation showed four phases that were influenced by precipitation events (an initial rapid increase followed by near stabilization), and responded little to precipitation events less than 1 mm.

Figure 10a shows that the daily actual evaporation showed peaks of 4.8, 5.7, 2.6, and 7.7 mm within 12 h after the rainfall events, versus respective values of 6.2, 5.3, 3.9, and 7.9 mm for pan evaporation. The rapid decline in evaporation that occurs after this initial peak, also known as the transition period (Wang et al. 2015), results from the decreased water supply created by the initial rapid evaporation, and creates an increasingly thick dry sand layer (to a depth of about 50 cm in the study area) that inhibits further water loss to some extent (Scanlon et al. 2010; Wang et al. 2015). During this stage, the actual evaporation rate decreased to less than 1 mm day^{-1} in the 1–2 days after the rainfall (Fig. 10a). Subsequently, the soil achieved a relatively

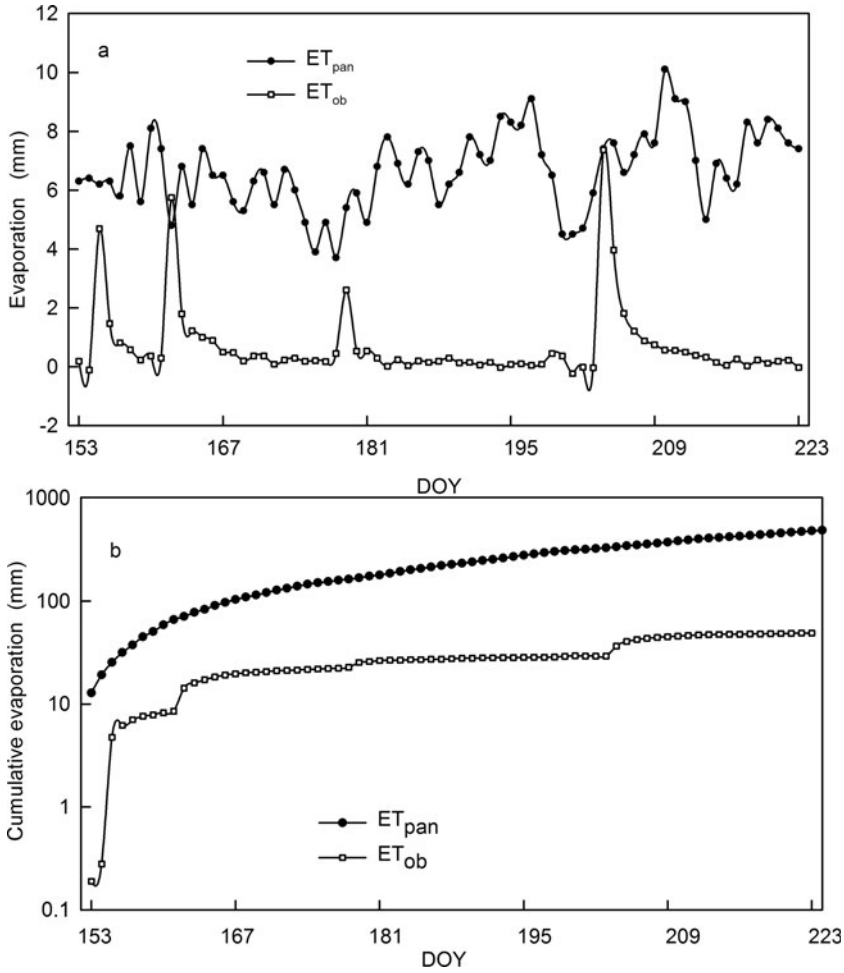

Fig. 10 Actual daily evaporation (ET_{ob}), and cumulative evaporation observed during the experimental period, compared to the pan evaporation (ET_{pan}). DOY, day of year

stable state with low evaporation, as in previous research (Ben Neriah et al. 2014; Lehmann et al. 2008; Shokri et al. 2009); that rate was approximately 0.2 mm day^{-1} in this study.

Potential recharge

Equation 1 produced a good linear regression between the water infiltration with a normal rainfall amount, and the infiltration (I_s) under the dry sand layer indicated by the potential recharge after this rainfall amount. Table 6 summarizes the results of the infiltration calculations to a depth of 50 cm based on the water balance equation after the three simulated and four natural rainfall events. There is no infiltration below the dry sand layer for rainfall less than 10 mm. Infiltration totaled only 0.013 mm with 21 mm of rainfall. Infiltration totaled 0.68 mm and penetrated to a depth below 50 cm with

Table 6 Water balance calculations during the three simulated (*M1*–*M3*; Table 3) and four natural (*N1*–*N4*; Table 5) rainfall events in the study area in 2014

Event No.	DOY	Range of infiltration depths (cm)	Rainfall (mm)	Pattern	I_s (mm)	ET_{ob} (mm)	ET_{pan} (mm)
M1	154	0–15	10	Normal	0	8.90	9.20
M2	162	0–30	21	Ordinary annual maximum	0.013	17.17	21.97
M3	204	>50	31	Extreme	0.68	29.71	34.03
N1	170	0–5	0.50	Normal	0	0.51	0.51
N2	174	0–5	3.35	Normal	0	3.30	3.30
N3	235	0–5	0.58	Normal	0	0.58	0.58
N4	236	0–5	0.25	Normal	0	0.25	0.25

DOY day of year; ET_{ob} observed actual evaporation; ET_{pan} daily pan evaporation

31 mm of rainfall, representing potential recharge equivalent to 1.7 % of the rainfall. This is comparable to the range of values (0.1–5.5 %) reported by other researchers (Ma and Edmunds 2006; Gates et al. 2008; Ma et al. 2009b, 2012; Scanlon et al. 2010); however, the recharge ratio would be several orders of magnitude smaller than 0.1 %.

Discussion

For rainfall to recharge groundwater, the wetting front must travel below the dry sand layer (De Vries et al. 2000; Scanlon et al. 2010). In these simulations, the infiltration depth reached only 30 cm below the soil surface even at a rainfall of 21 mm (Fig. 7); this means that 92.4 % of the rainfall events in the study area (Table 1) cannot produce groundwater recharge, that the existence of the dry sand layer creates a barrier to the advancing wetting front, and that most of the rainfall evaporates. Similar results were reported in China in the Badain Jaran Desert (Ma et al. 2014) and the Tengger Desert (Chen et al. 2014); however, after extreme rainfall events, the dry sand layer cannot intercept all of the rainfall infiltration. Figure 6 clearly indicates that the wetting front infiltrates to a depth of at least 50 cm within 12 h after the occurrence of a 31-mm rainfall event. These results may therefore explain why the potential recharge is low in other desert regions with a dry sand layer that is thicker than 20 cm (Ma et al. 2014).

It is unclear whether the potential recharge after the rainfall events can be used as an important factor to identify the occurrence of groundwater recharge (De Vries et al. 2000; Dong et al. 2013). Evaporation is a key factor that determines the water available for infiltration and must be accurately estimated to calculate the water balance of a soil (Romano and Giudici 2009; Salih and Sendil 1984; Solaiman and Abdin 1987). The differences in SWC to a depth of 50 cm in the soil profile played a significant role in rainfall infiltration during the initial stages of rainfall events, both in the present study and in previous studies (Ritsema and Dekker 1994; Wang et al. 2008). For rainfall to affect the layer of wet sand below the surface dry sand layer, it must first infiltrate past the dry layer. When it does so, it can contribute directly to maintaining the wet sand layer, as was found in a study of a megadune (Wen et al. 2014), and it can be responsible for potential recharge of groundwater; however, there is a time lag between the potential recharge and actual groundwater recharge (De Vries and Schwan 2000; De Vries et al. 2000; Huang et al. 2013).

The daily pan evaporation (i.e., potential evaporation) averaged 7.2 mm during the experiment period, which represents extremely strong evaporation compared with the normal and ordinary annual maximum precipitation. For potential recharge to occur, the amount of water that enters the soil must be greater than this evaporation rate, and it must infiltrate the dry soil sufficiently rapidly that it overcomes the inhibition effect (i.e., a barrier to further evaporation) created by the dry sand layer; the inhibition effect will prevent further evaporation and allow infiltration to continue when the water reaches this depth.

The present results show how accurate dynamic monitoring of changes in moisture content is required to understand the roles of the dry sand layer in infiltration and evaporation. This analysis shows that potential recharge did not occur at normal and ordinary annual maximum rainfall magnitudes, but that a potential recharge of 0.68 mm occurred with 31 mm of rainfall (Table 6). Because of the limited frequency of rainfall events that would permit potential recharge and a lack of continuous observation over a range of observation depths, the contribution of this small recharge amount has generally been ignored by previous researchers. Discussions with other researchers who have performed work in the study area suggests that no runoff is produced in this extremely arid area; thus, the precipitation is consumed primarily by evaporation (because there is little or no vegetation cover in this region to cause transpiration loss), with only a small proportion potentially recharging the groundwater. In other words, the precipitation equals the actual evaporation during individual normal and ordinary annual maximum rainfall events because the dry sand layer creates a barrier to infiltration of water to a depth that would prevent further evaporation; thus, only extreme precipitation events offer the possibility of recharge of groundwater in this extremely arid area.

Conclusions

The present study investigated the effect of the surface dry sand layer on groundwater recharge using three levels of simulated rainfall (normal, ordinary annual maximum, and extreme) that were based on historical rainfall data for this study area. The major conclusions are following:

1. The analyses of both simulated and natural rainfall events revealed that most of the water movement in the sandy soil occurred within the top 20 cm of the soil. Soil moisture did not change below this depth for 92.4 % of the rainfall events in this study area. These results suggest that rainfall events greater than 30 mm are required for water to infiltrate sufficiently deeply to potentially recharge the groundwater.
2. The strong evaporative demand in the study area has created a thick layer of dry sand, reaching up to 50 cm in depth, in this study area. This layer affects groundwater in complex ways; for example, this layer prevents deep infiltration of most rainfall, because the evaporation rate is greater than the infiltration rate produced by low-rainfall events. However, water that penetrates sufficiently deep

into this layer is subsequently protected from evaporation, and as a result, it can continue moving downwards and potentially recharge the groundwater.

Acknowledgements This work was supported by the National Natural Science Foundation of China (41271039) and the Fundamental Research Funds for the Central Universities (lzujbky-2014-263). We thank the Dunhuang Meteorological Station for providing the meteorological data and Dunhuang Field Scientific Exprimental Station of Lanzhou University for simulating and observation in this study. We would like to thank two anonymous reviewers and associate editor, John B Gates for their comments that have led to improvements in the paper. We also thank Dr. Martin Appold (editor) and Ms. Sue Duncan (technical editorial advisor) for their continued help during the revisions of the paper.

References

Ahn S, Im S, Doerr S (2012) Effect of thickness of a water repellent soil layer on soil evaporation rate. In: Proceedings of the EGU General Assembly, Vienna, Austria, European Geosciences Union, Munich, Germany, pp 22–27

Allen RG, Pereira LS, Raes D, Smith M (1998) Crop evapotranspiration guidelines for computing crop water requirements. FAO Irrigation and Drainage Paper 56, Food and Agriculture Organization, Rome

Ben Neriah A, Assouline S, Shavit U, Weisbord N (2014) Impact of ambient conditions on evaporation from porous media. Water Resour Res 50:6696–6712. doi:10.1002/2014WR015523

Brutsaert W (2014) Daily evaporation from drying soil: universal parameterization with similarity. Water Resour Res 50:3206–3215. doi:10.1002/2013WR014872

Chen JS, Chen XX, Wang T (2014) Isotopes tracer research of wet sand layer water sources in Alxa Desert (in Chinese). Adv Water Sci 25(2):196–206

De Vries JJ, Schwan J (2000) Groundwater flow and geological structure of the Algarve, Portugal. Faculty of Earth Sciences, Vrije Universiteit, Amsterdam, 104 pp

De Vries JJ, Simmers I (2002) Groundwater recharge: an overview of processes and challenges. Hydrogeol J 10:5–17. doi:10.1007/s10040-001-0171-7

De Vries JJ, Selaolo ET, Beekman HE (2000) Groundwater recharge in the Kalahari, with reference to paleo-hydrologic conditions. J Hydrol 238:110–123. doi:10.1016/S0022-1694(00)00325-5

Dong ZB, Qian GQ, Lv P, Hu G (2013) Investigation of the sand sea with the tallest dunes on Earth: China's Badain Jaran Sand Sea. Earth Sci Rev 120:20–39. doi:10.1016/j.earscirev.2013.02.003

Edmunds WM, Ma JZ, Aeschbach-Hertig W, Kipfer R, Darbyshire DPF (2006) Groundwater recharge history and hydrogeochemical evolution in the Minqin Basin, North West China. Appl Geochem 21:2148–2170. doi:10.1016/j.apgeochem.2006.07.016

Fan Y, Li H, Miguez-Macho G (2013) Global patterns of groundwater table depth. Science 339(6122):940–943. doi:10.1126/science.1229881

Fritton DD, Kirkham D, Shaw RH (1967) Soil water chloride redistribution under various evaporation potentials. Soil Sci Soc Am Proc 31:599–603. doi:10.2136/sssaj1967.03615995003100050002x

Gates JB, Edmunds WM, Ma JZ, Scanlon BR (2008) Estimating groundwater recharge in a cold desert environment in northern China using chloride. Hydrogeol J 16:893–910. doi:10.1007/s10040-007-0264-z

Goss KU, Madliger M (2007) Estimation of water transport based on in situ measurements of relative humidity and temperature in a dry Tanzanian soil. Water Resour Res 43:W05433. doi:10.1029/2006WR005197

Huang TM, Pang ZH, Edmunds WM (2013) Soil profile evolution following land-use change: implications for groundwater quantity and quality. Hydrol Process 27:1238–1252. doi:10.1002/hyp.9302

Lehmann P, Assouline S, Or D (2008) Characteristic lengths affecting evaporative drying of porous media. Phys Rev E 77. doi:10.1103/PhysRevE.77.056309

Liu H, Lei TW, Zhao J, Yuan CP, Fan YT, Qu LQ (2011) Effect of rainfall intensity and antecedent soil water content on soil infiltrability under rainfall conditions using the run off-on-out method. J Hydrol 396:24–32. doi:10.1016/j.jhydrol.2010.10.028

Liu XP, He YH, Zhang TH, Zhao XY, Li YQ, Zhang LM, Wei SL, Yun JY, Yue X (2015) The response of infiltration depth, evaporation, and soil water replenishment to rainfall in mobile dunes in the Horqin Sandy Land, northern China. Environ Earth Sci 73:8699–8708. doi:10.1007/s12665-015-4125-0

Ma J, Edmunds WM (2006) Groundwater and lake evolution in the Badain Jaran desert ecosystem, Inner Mongolia. Hydrogeol J 14:1231–1243. doi:10.1007/s10040-006-0045-0

Ma J, Ding ZY, Edmunds WM, Gates JB, Huang TM (2009a) Limits to recharge of groundwater from Tibetan plateau to the Gobi Desert, implication for water management in the mountain front. J Hydrol 364:128–141. doi:10.1016/j.jhydrol.2008.10.010

Ma J, Edmunds WM, He JH, Jia B (2009b) A 2000 year geochemical record of palaeoclimate and hydrology derived from dune sand moisture. Palaeogeogr Palaeoclimatol Palaeoecol 276:38–46. doi:10.1016/j.palaeo.2009.02.028

Ma J, Wang YQ, Zhao YP (2012) Spatial distribution of chloride and nitrate within an unsaturated dune sand of a cold-arid desert: implications for paleoenvironmental records. Catena 96:68–75. doi:10.1016/j.catena.2012.04.012

Ma J, He JH, Qi S (2013) Groundwater recharge and evolution in the Dunhuang Basin, northwestern China. Appl Geochem 28:19–31. doi:10.1016/j.apgeochem.2012.10.007

Ma N, Wang NA, Zhao LQ (2014) Observation of mega-dune evaporation after various rain events in the hinterland of Badain Jaran desert. Chin Sci Bull 59:162–171. doi:10.1007/s11434-013-0050-3

Ritsema CJ, Dekker LW (1994) How water moves in a water repellent sandy soil: dynamics of fingered flow. Water Resour Res 30(9):2519–2531. doi:10.1029/94WR00750

Romano E, Giudici M (2009) On the use of meteorological data to assess the evaporation from a bare soil. J Hydrol 372:30–40. doi:10.1016/j.jhydrol.2009.04.003

Salih A, Sendil U (1984) Evapotranspiration under extremely arid climates. J Irrig Drain Eng 110:289–303

Scanlon BR, Mukherjee A, Gates J (2010) Groundwater recharge in natural dune systems and agricultural ecosystems in the Thar Desert region, Rajasthan, India. Hydrogeol J 18:959–972. doi:10.1061/(ASCE)0733-9437(1984)110:3(289)

Schindewolf M, Schmidt J (2012) Parameterization of the EROSION 2D/3D soil erosion model using a small-scale rainfall simulator and upstream runoff simulation. Catena 91:47–55. doi:10.1016/j.catena.2011.01.007

Shahraeeni E, Lehmann P, Or D (2012) Coupling of evaporative fluxes from drying porous surfaces with air boundary layer: characteristics of evaporation from discrete pores. Water Resour Res 48:9525. doi:10.1029/2012WR011857

Shokri NP, Lehmann P, Or D (2009) Critical evaluation of enhancement factors for vapor transport through unsaturated porous media. Water Resour Res 45:W10433. doi:10.1029/2009WR007769

Shurbaji AR, Campbell AR (1997) Study of evaporation and recharge in desert soil using environmental tracers, New Mexico, USA. Environ Geol 29(3–4):147–151. doi:10.1007/s002540050112

Solaiman AA, Abdin MAS (1987) Evapotranspiration estimates in extremely arid areas. J Irrig Drain Eng 113:565–574. doi:10.1061/(ASCE)0733-9437(1987)113:4(565)

Swenson SC, Lawrence DM (2014) Assessing a dry surface layer-based soil resistance parameterization for the Community Land Model using GRACE and FLUXNET-MTE data. J Geophys Res Atmos 119(17):10299–10312. doi:10.1002/2014JD022314

Vörösmarty CJ, Green P, Salisbury J, Lammers RB (2000) Global water resources: vulnerability from climate change and population growth. Science 289:284–288. doi:10.1126/science.289.5477.284

Wada Y, van Beek LPH, van Kempen CM, Reckman JWTM, Vasak S, Bierkens MFP (2010) Global depletion of groundwater resources. Geophys Res Lett 37(20). doi:10.1029/2010GL044571

Wang XX (2015) Vapor flow resistance of dry soil layer to soil water evaporation in arid environment: an overview. Water 7:4552–4574. doi:10.3390/w7084552

Wang XP, Kang ES, Zhang JG, Li XR (2004) Evapotranspiration of *Artemisia ordosia* vegetation in stabilized arid desert dune in Shapotou, China. Arid Land Res Manag 18:63–76. doi:10.1080/15324980490245022

Wang XP, Zhang TH, Zhao HL, Yue GY (2006) Infiltration and redistribution process of rainfall in desert mobile sand dune. J Hydraul Eng 37(2):166–171. doi:10.1002/hyp.9767

Wang XP, Cui Y, Pan YX, Li XR (2008) Effects of precipitation characteristics on infiltration and redistribution patterns in revegetation-stabilized desert ecosystems. J Hydrol 358:134–143. doi:10.1016/j.jhydrol.2008.06.002

Wang H, Gao JE, Zhang MJ, Li XH, Zhang SL, Jia LZ (2015) Effects of rainfall intensity on groundwater recharge based on simulated rainfall experiments and a groundwater flow model. Catena 127:80–91. doi:10.1016/j.catena.2014.12.014

Wen J, Su ZB, Zhang TT, Tian H, Zeng YJ, Liu R, Kang Y, van der Velde R (2014) New evidence for the links between the local water cycle and the underground wet sand layer of a mega-dune in the Badain Jaran Desert, China. J Arid Land 6(4):371–377. doi:10.1007/s40333-014-0062-0

Wu Z (2009) Sandy deserts and its control in China. Science Press, Beijing

Xie XQ, Wang L (2007) Changes of potential evaporation in northern China over the past 50 years (in Chinese). J Nat Resour 22(5):683–691

Xu XY, Zhang RD, Xue XZ, Zhao M (1998) Determination of evapotranspiration in the desert area using lysimeters. Commun Soil Sci Plant Anal 29(1-2):1–13. doi:10.1080/00103629809369924

Yamanaka T, Yonetani T (1999) Dynamics of the evaporation zone in dry sandy soils. J Hydrol 217:135–148. doi:10.1016/S0022-1694(99)00021-9

Yamanaka T, Takeda A, Sugita F (1997) A modified surface resistance approach for representing bare-soil evaporation: wind tunnel experiments under various atmospheric conditions. Water Resour Res 33(9):2117–2128. doi:10.1029/97WR01639

Yang WB, Tang JN, Liang HR, Dang HZ, Li W (2014) Deep soil water infiltration and its dynamic variation in the shifting sandy land of typical deserts in China. Sci China Earth Sci 57(8):1816–1824. doi:10.1007/s11430-014-4882-8